Clinical Radiology xxx (xxxx) xxx

Contents lists available at ScienceDirect

Clinical Radiology

journal homepage: www.clinicalradiologyonline.net

Pancreatic fibrosis assessment and association with pancreatic cancer: comparison with the extracellular volume fraction

H. Fukui [1,*], H. Onishi [1], T. Ota [1], A. Nakamoto [1], T. Tsuboyama [1], Y. Enchi [3], D. Yamada [2], Y. Takeda [2], S. Kobayashi [2], Y. Fukuda [2,4], H. Eguchi [2], T. Matsui [5], M. Tatsumi [1], N. Tomiyama [1]

[1)] *Department of Diagnostic and Interventional Radiology, Osaka University Graduate School of Medicine, Japan*
[2)] *Department of Gastroenterological Surgery, Osaka University Graduate School of Medicine, Japan*
[3)] *Division of Radiology, Department of Medical Technology, Osaka University Hospital, Japan*
[4)] *Department of Gastroenterological Surgery, Kindai University Nara Hospital, Japan*
[5)] *Department of Pathology, Osaka University Graduate School of Medicine, Japan*

ARTICLE INFORMATION

Article history:
Received 1 May 2024
Received in revised form
1 July 2024
Accepted 6 August 2024

AIMS: To compare the iodine washout rate (IWR) from multiphasic contrast-enhanced computed tomography (CT) with the extracellular volume fraction (fECV) for assessing pancreatic fibrosis and its association with pancreatic cancer.

MATERIALS AND METHODS: The study included 51 individuals (33 men; median age: 69 years; 21 with pancreatic cancer, 30 with other diseases) who underwent multiphasic contrast-enhanced CT and histological evaluation for fibrotic changes in pancreas. The histological pancreatic fibrosis fraction (HPFF) was assessed on Azan-stained sections. Pancreatic parenchymal enhancement values were measured to calculate IWR and fECV. Statistical methods, such as Spearman's rho and Mann–Whitney *U*-test, were used. Linear regression models using IWR and fECV were constructed to predict HPFF, with the performance expressed as root mean squared error (RMSE) and Akaike information criterion (AIC).

RESULTS: HPFF correlated with all CT parameters at the estimated transection line, strongest for IWR_{PPP-EP} ($r=-0.69$, $P<0.01$). HPFF and fECV values were higher in the pancreatic cancer group than in controls (30% vs. 12.5%, $P<0.01$; 40.3% vs. 33.0%, $P<0.01$), whereas IWR values were lower (IWR_{PPP-EP}: 43.3% vs. 55.0%, $P<0.01$; IWR_{PVP-EP}: 25.0% vs. 33.5%, $P<0.01$). Linear regression models combining IWR_{PPP-EP} + fECV and IWR_{PVP-EP} + fECV were superior for predicting HPFF, with lower RMSE (9.23–9.35) and AIC (379.38–380.72) values than models with IWR or fECV alone.

CONCLUSION: IWR_{PPP-EP}, IWR_{PVP-EP}, and fECV were reliable biomarkers for noninvasively assessing pancreatic fibrosis and were associated with pancreatic cancer risk. Linear regression combining these variables showed enhanced predictive accuracy for pancreatic fibrosis.

Abbreviations: IWR, Iodine washout rate; fECV, Extracellular volume fraction; SSIM, SURE SUBTRACTION Iodine Mapping; ROC, Receiver operating characteristic; ROI, Region of interest; AUC, Area under the curve; HPFF, Histological pancreatic fibrosis fraction; RMSE, Root mean squared error; AIC, Akaike information criterion; ICC, Intraclass correlation coefficient.

* Guarantor and correspondent: Hideyuki Fukui, Department of Diagnostic and Interventional Radiology, Osaka University Graduate School of Medicine, D1, 2-2, Yamadaoka, Suita, Osaka 565-0871, Japan.
E-mail address: hidefukui@infoseek.jp (H. Fukui).

https://doi.org/10.1016/j.crad.2024.08.007

Please cite this article as: Fukui H et al., Pancreatic fibrosis assessment and association with pancreatic cancer: comparison with the extracellular volume fraction, Clinical Radiology, https://doi.org/10.1016/j.crad.2024.08.007

Introduction

Assessment of pancreatic fibrosis is crucial for diagnosing, staging, and managing pancreatic diseases.[1–3] Traditional methods of evaluating pancreatic fibrosis involve invasive procedures, such as pancreatic biopsy, which have several limitations and risks. Therefore, significant attention has recently been given to developing noninvasive imaging techniques for assessing pancreatic fibrosis.

In recent years, the extracellular volume fraction (fECV) has emerged as an imaging biomarker for characterizing pancreatic fibrosis.[4,5] The fECV was calculated from the enhancement values on the computed tomography (CT) images acquired during the equilibrium phase and the hematocrit values of the blood and quantifies the extracellular space within a tissue compartment, reflecting the accumulation of extracellular matrix components associated with fibrosis. Several studies have demonstrated the potential of fECV measurements for differentiating pancreatic fibrosis from normal pancreatic tissue and monitoring disease progression.[4–8]

The area of contrast accumulation in the tissue on biphasic contrast-enhanced CT can also accurately evaluate fibrosis in pancreas and prognose a clinically relevant anastomotic failure after pancreatoduodenectomy.[9] Recently, it has been reported that the iodine washout rate (IWR), an indicator of the enhancement pattern, predicts liver fibrosis more accurately than fECV in multiphasic CT.[10] However, as far as we know, it has not yet been elucidated, which measure, IWR or ECV, is more accurate for assessing pancreatic fibrosis and their respective associations with pancreatic cancer.

Therefore, the primary study objective was to compare the utility of IWR determined by multiphasic contrast-enhanced CT with that of fECV for assessing pancreatic fibrosis. We also investigated the association between these imaging biomarkers and pancreatic cancer, to better understand the complex interplay between pancreatic fibrosis and malignancy. A key aspect of our methodology was to develop and assess multiple linear regression models that combined the IWR and fECV for assessing pancreatic fibrosis. The overall goal was to improve the predictive accuracy of these noninvasive imaging techniques for evaluating pancreatic fibrosis and its potential link to pancreatic malignancies, enabling earlier detection.

Materials and methods

The research received approval from the Institutional Review Board of Osaka University Hospital (approval number 20351) along with the waiver for informed consent.

Patients

The study participants were the same as those in our previous study ("Pancreatic Fibrosis by Extracellular Volume Fraction Using Contrast-Enhanced Computed Tomography and Relationship with Pancreatic Cancer" by Fukui H et al., 2022). We evaluated 333 consecutive patients subjected to pancreatectomy at our clinical setting between January 2014 and May 2019. To ensure consistency, we applied inclusion criteria similar to those of a previous study. Patients meeting the following criteria were included in the analysis: (1) had undergone preoperative multiphasic contrast-enhanced CT, covering nonenhanced, pancreatic parenchymal, portal venous, and equilibrium phase CT, and (2) had not undergone presurgical therapeutic treatment before CT. Consequently, we excluded 202 individuals without preoperative unenhanced and equilibrium contrast-enhanced CT imaging and 19 patients who underwent preoperative therapy before CT. Among the other 112 individuals, 16 with atrophic changes were detected during diagnostic imaging that were accompanied by significant dilation of pancreatic ducts and 8 with signs of acute pancreatitis on CT images or laboratory tests were not included in the sample.[11] Further exclusions were made on the basis of specific criteria. In total, 24 patients received preoperative therapy after CT, 12 had nontumorous parenchyma of pancreas that could not be histologically assessed, and 1 encountered an unknown error preventing the creation of subtraction images. Consequently, 51 resected specimens were available for assessing pathological pancreatic conditions in noncancerous lesions. Among the 51 patients from whom the specimens were taken, 25 underwent pancreaticoduodenectomy, 24 underwent distal pancreatectomy, and 2 were subjected to central pancreatectomy. Based on the outcomes of a pathological examination, the patients were assigned to two groups: pancreatic cancer (n=21) and the nonaffected (n=30). Additionally, the patients were further divided into two subgroups: those with diabetes mellitus (DM) (n=21) and without DM (n=30) diagnosed according to the classification and diagnostic criteria for DM by the American Diabetes Association (Fig 1).[12] The median interval between the intervention and obtaining CT diagnostic images was 49 days (2−294 days).

Pathological examination

For a retrospective analysis, Azan-saturated, 2-μm-thick sections were received from the resected pancreatic material, with a minimum distance of 15 mm from the pathologic formations to minimize interaction with the affected malignant tissues.[5,13] The slides were examined by a light

Please cite this article as: Fukui H et al., Pancreatic fibrosis assessment and association with pancreatic cancer: comparison with the extracellular volume fraction, Clinical Radiology, https://doi.org/10.1016/j.crad.2024.08.007

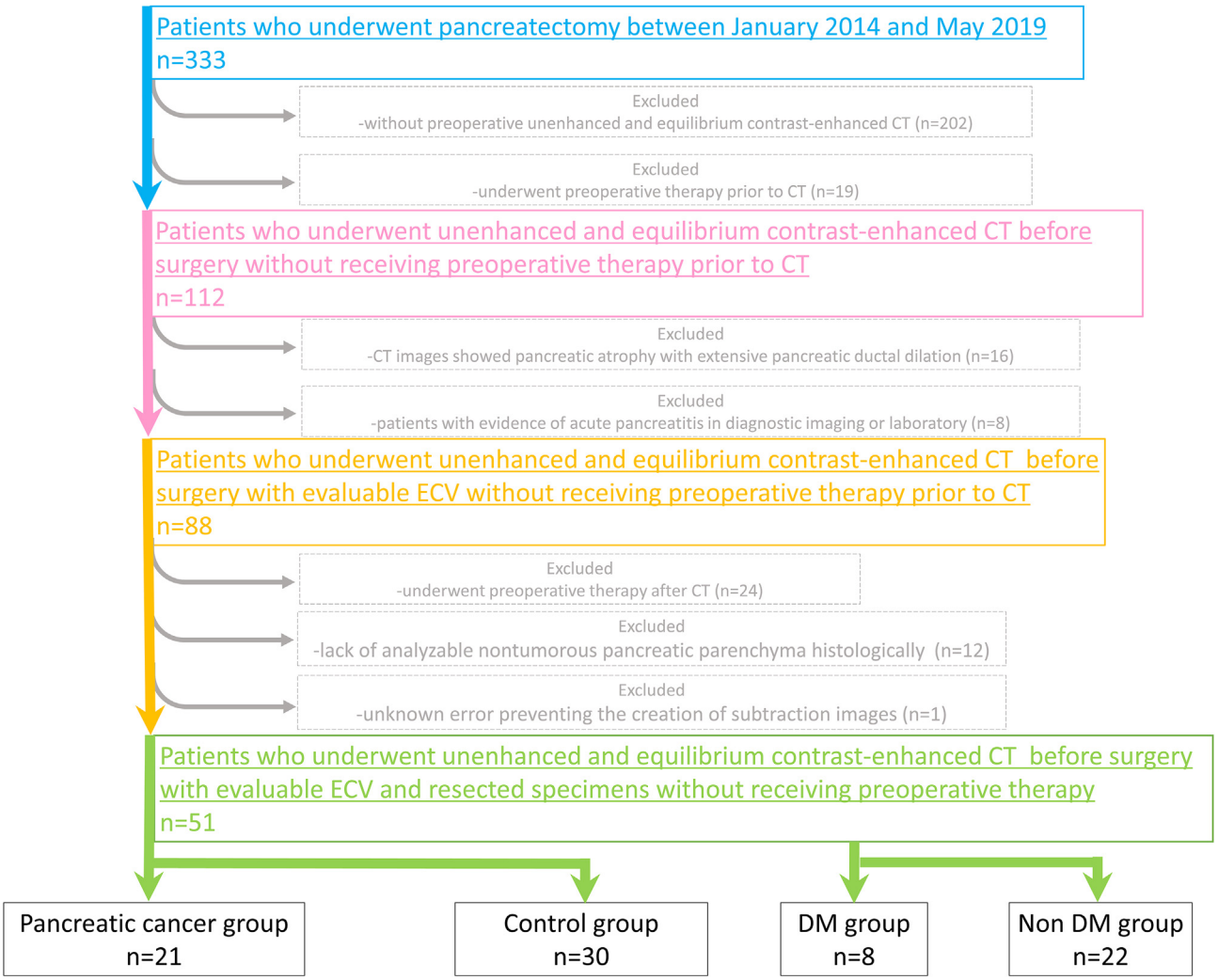

Figure 1 Study flowchart.

microscope (BZ-X800; Keyence, Osaka, Japan). To maintain objectivity, the investigators blinded to the IWR, fECV, and clinical data performed the analysis. Different areas of interest were detected, and the image joint function was used to seamlessly combine these areas into a single image.[14] The entire slide was thoroughly examined by an investigator under the supervision of expert pathologists from our institution. To assess the histological pancreatic fibrosis fraction (HPFF), ×100 microscopic images of nonaffected tissues of pancreas were used. Image assessment software (BZ-X analyzer; Keyence, Osaka, Japan) was used to measure the extent of histological pancreatic fibrosis at the resection stump.[15] The software included an automated fibrosis selection function based on color contrast that allowed accurate area calculations. HPFF was outlined as the percentage of fibrosis within the parenchyma of pancreas (excluding unfilled anatomic formations like lumens of vessels) (Fig 2a).

CT imaging

Either a 320- (Aquilion One Genesis Edition; Canon Medical Systems, Otawara, Japan), a 160- (Aquilion Precision; Canon Medical Systems), or a 64-channel multislice CT scanner (Discovery CT 750 HD or Discovery CT 750 HD Freedom Edition; GE Healthcare) was used for CT imaging. The evaluation parameters were the following: collimation, 0.625 × 64 or 0.5 × 80 mm^3; pitch, 1.375 or 0.813 mm/rotation; rotation time, 0.4 or 0.5 s/rotation; exposure parameters of 120 kV and autoexposure control with a noise index SD of 13.8 or 15; and field of view, 345 mm. After obtaining the precontrast scan, pancreatic parenchymal phases (PPP) were acquired using the bolus-tracking technique 20 s after achieving 100-HU attenuation of the descending aorta. Portal-venous phases (PVP) were obtained 35 s after PPP acquisition, and equilibrium phases (EP) were visualized 120 s after PVP acquisition. Intravenous administration of contrast medium with iodine 600 mg I/kg body weight was done for 30 s. A new subtraction algorithm (SURE SUBTRACTION Iodine Mapping (SSIM), Canon Medical Systems, Tokyo, Japan) was applied to acquire subtraction images between the nonenhanced and all phases of dynamic contrast.[16]

Please cite this article as: Fukui H et al., Pancreatic fibrosis assessment and association with pancreatic cancer: comparison with the extracellular volume fraction, Clinical Radiology, https://doi.org/10.1016/j.crad.2024.08.007

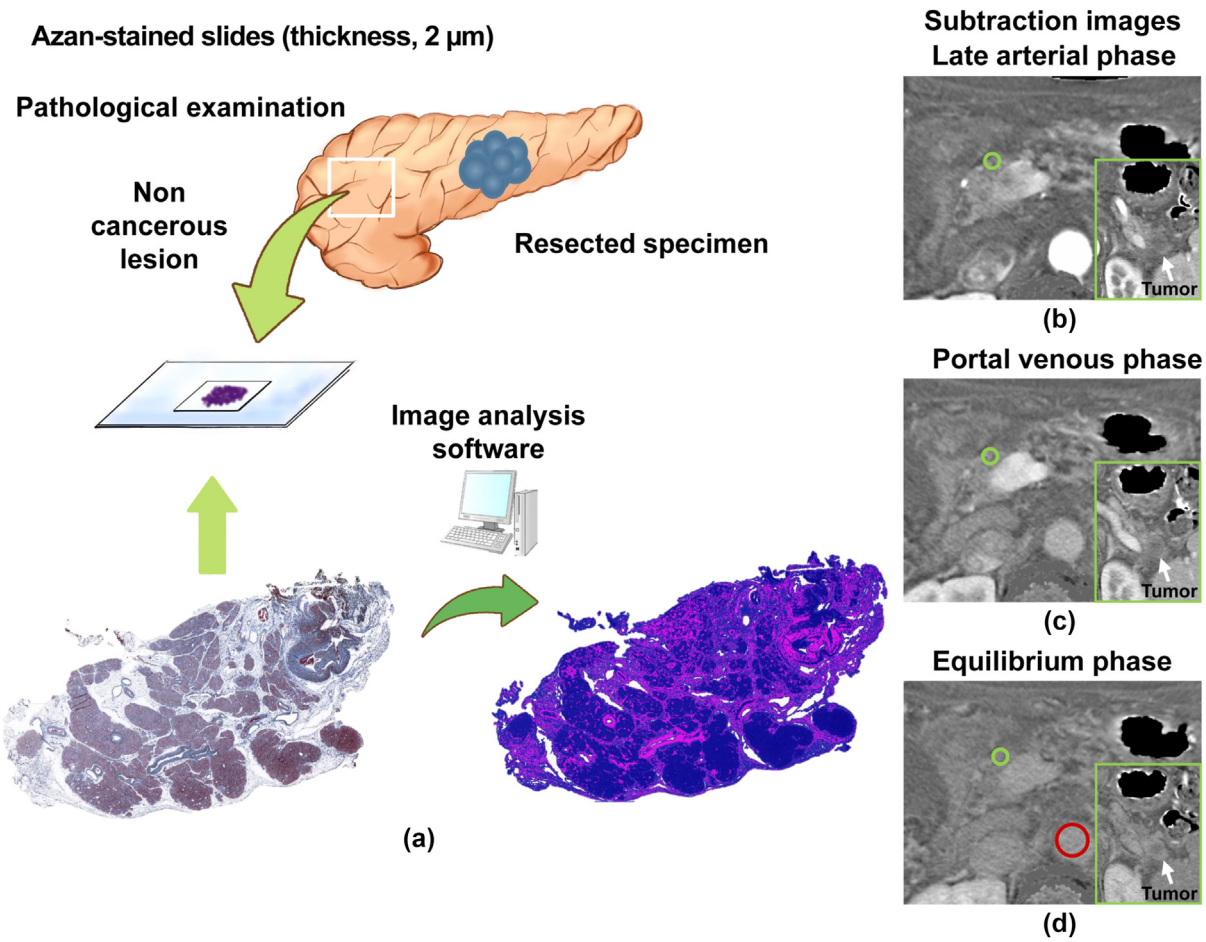

Figure 2 Images from a 69-year-old male patient who was subjected to distal pancreatectomy for cancer of pancreas. (a) Azan-stained specimen scanned with a slide-scanning microscope showing areas of fibrosis. Image analysis software was used to calculate the ratio of the fibrotic areas in the pancreatic parenchyma (the ratio was 24.0% in this patient). After generating subtraction images by subtracting unenhanced CT images from the PPP, PV, and EP images using a nonrigid correction technique (b)–(d), pancreatic parenchymal enhancement values were measured in each phase, and the IWRs and fECV were calculated. In this patient, the $IWR_{PPP-PVP} = 9.67\%$, $IWR_{PPP-EP} = 36.4\%$, $IWR_{PVP-EP} = 29.6\%$, fECV = 37.1%, $IWR_{PPP-PVP}$ + fECV model = 23.4%, IWR_{PPP-EP} + fECV model = 27.1%, and IWR_{PVP-EP} + fECV model = 21.5%. *PPP* (pancreatic parenchymal phase), *PVP* (portal-venous phase), *EP* (equilibrium phase), *IWR* (iodine washout rate), and *fECV* (extracellular volume fraction).

Quantitative analysis of images

IWR and fECV evaluations were done manually on an image workstation (Synapse; Fujifilm, Tokyo, Japan). To estimate the extent of enhancement (in Hounsfield units) of pancreatic parenchyma (ΔPancreas), two board-certified abdominal radiologists, with 12 and 28 years of experience, accurately positioned the greatest available region of interest (ROI) in the form of an ellipse on a pancreas at a suggested transverse section line to align the areas of interest on SSIM-subtracted images with those defined by a pathological examination.[5,13] A consultation with a surgeon was done if there were uncertainties about the transection line on radiological assessment. We established the ROI away from the indicated line to detect variations in the IWR and fECV for sites at and away from the latter. To determine the extent of enhancement of the aorta (ΔAorta) and portal vein (ΔPortal), ROIs were outlined as the largest possible areas in the lumens of the aorta and portal vein and not covering a vessel wall. Another radiologist with 12 years of experience positioned ROIs to achieve interobserver reliability, and the blinding of clinical data was done. The ΔAorta and ΔPortal of each individual were comparatively analyzed to ensure adequate acquisition of an equilibrium phase. If significant differences between ΔAorta and ΔPortal (>±10 HU) were found, they were regarded as outliers and eliminated.[17] The IWR and fECV were measured with the following equation: $IWR_{PPP-EP} = (1 - \Delta Pancreas_{EP}/\Delta Pancreas_{PPP}) \times 100$, $IWR_{PVP-EP} = (1 - \Delta Pancreas_{EP}/\Delta Pancreas_{PVP}) \times 100$, $IWR_{PPP-PVP} = (1 - \Delta Pancreas_{PV}/\Delta Pancreas_{PPP}) \times 100$ and $fECV = (100 - \text{hematocrit}) \times \Delta Pancreas_{EP}/\Delta Aorta_{EP}$.[4,5,10] The laboratory blood test results obtained at the nearest date of CT imaging were chosen for the assessment (median, 6 ± 5 days; range, 0–54 days) (Fig 2b–2d).

Statistical analysis

The Shapiro–Wilk test was carried out to outline normal distribution. Pearson's correlation coefficient and two-sample *t*-test were applied pairwise, except for the

Please cite this article as: Fukui H et al., Pancreatic fibrosis assessment and association with pancreatic cancer: comparison with the extracellular volume fraction, Clinical Radiology, https://doi.org/10.1016/j.crad.2024.08.007

Table 1
Patient characteristics.

Characteristic	Value
No. of patients	51
Age (y)[a]	61 (17–84)
No. of female patients	18 (35.3)
No. of male patients	33 (64.7)
BMI (kg/m^2)[a]	21.7 (14.7–32.4)
Drinking	15 (29.4)
Smoker	20 (39.2)
Diabetes mellitus	21 (41.2)
Purpose of contrast-enhanced CT	
Pancreatic cancer	21 (41.2)
Cholangiocarcinoma	10 (19.6)
Intraductal papillary mucinous adenoma	7 (13.7)
Branch duct	0 (0)
Main duct	1 (2.0)
Mixed	6 (6.9)
Neuroendocrine tumor	2 (3.9)
Solid pseudopapillary neoplasm	6 (11.8)
Ampullary cancer	1 (2.0)
Pancreatic intraepithelial neoplasia	2 (3.9)
Epidermoid cyst	1 (2.0)
Pancreatic arteriovenous malformation	1 (2.0)

BMI (body mass index), *CT* (computed tomography).
Note: Unless otherwise indicated, data are numbers of patients (n=51), with percentages in parentheses.
[a] Data are medians and ranges in parentheses.

correlation and differences between fECV at and away from the evaluated transverse section line, where Spearman's rank correlation coefficient and Mann–Whitney *U*-test were applied for the analysis. We used the Meng–Rosenthal–Rubin method to detect statistically significant differences between the correlation coefficients.[18] Considering the analysis of $IWR_{PPP-PVP}$, IWR_{PPP-EP}, IWR_{PVP-EP}, and fECV, a two-sample *t*-test was carried out to assess the differences between the two groups. Additionally, for the analysis of HPFF, the Mann–Whitney *U*-test was performed for the indicated groups. Multiple linear regression models incorporating the predictor variable fECV along with $IWR_{PPP-PVP}$, IWR_{PPP-EP}, IWR_{PVP-EP}, and fECV were constructed. The dependent variable was HPFF. The general form of the linear regression equation was as follows:

$$\text{Estimated HPFF} = \beta 0 + \beta 1(\text{IWR}) + \beta 2(\text{fECV})$$

where β0 is the intercept, and β1 and β2 are the coefficients associated with each predictor.

We used the AIC and RMSE to analyze the performance of each model.[19,20] The former was used to evaluate the compromise between model fit and complexity, with lower AIC values correlating positively with a better fit. RMSE was used to quantify the predictive accuracy of each model. To assess the potential influence of DM on the performance of the linear regression models for predicting HPFF, we used the RMSE and AIC to evaluate the performance of each linear regression model ($IWR_{PPP-PVP}$ + fECV, IWR_{PPP-EP} + fECV, IWR_{PVP-EP} + fECV, $IWR_{PPP-PVP}$, IWR_{PPP-EP}, IWR_{PVP-EP}, and fECV) in both groups. Receiver operating characteristic (ROC) analysis was carried out to determine the optimal cutoff values according to Youden index.[21] This analysis encompassed the $IWR_{PPP-PVP}$, IWR_{PPP-EP}, IWR_{PVP-EP}, fECV, and linear regression models. For all tests, $P<0.05$ was accepted as indicating significance. The values for the intraclass correlation coefficient (ICC) for interobserver agreement were determined. Bland–Altman analysis was also carried out.[22] An |R| value of ≤0.19 indicated a very weak correlation, 0.20–0.39 reflected a weak, 0.40–0.59 showed a moderate, 0.60–0.79 represented a strong, and 0.80–1.00 displayed a very strong one. EZR version 1.50 software (Saitama Medical Center, Jichi Medical University) was performed for all statistical analyses.

Table 3
Correlation coefficients between HPFF and CT parameters and comparison of these parameters between the pancreatic cancer and control groups.

Measure	Correlation with HPFF at transverse section line	Pancreatic cancer group	Control group	P-value
HPFF	/	30% (IQR, 18.0%–37.0%)	12.5% (IQR, 8–16.75%)	<0.01
$IWR_{PPP-PVP}$	−0.48	25.1% (SD 12.5)	32.1% (SD 12.8)	<0.05
IWR_{PPP-EP}	−0.69	43.3% (SD 14.3)	55.0% (SD 10.4)	<0.01
IWR_{PVP-EP}	−0.61	25.0% (SD 10.1)	33.5% (SD 8.74)	<0.01
fECV	−0.65	40.3% (SD 8.40)	33.0% (SD 5.82)	<0.01

fECV (extracellular volume fraction), *HPFF* (histological pancreatic fibrosis fraction), *IWR* (iodine washout rate), *IQR* (interquartile range), *SD* (standard deviation), *PPP* (pancreatic parenchymal phase), *PVP* (portal venous phase), *EP* (equilibrium phase).

Results

The features of the studied sample are summarized in Table 1. The ICCs and Bland–Altman analysis results for $IWR_{PPP-PVP}$, IWR_{PPP-EP}, IWR_{PVP-EP}, and fECV at away from the evaluated transverse section line are presented in Table 2. The ICCs ranged from 0.68 to 0.89, indicating good reproducibility for all measurements at both locations. Bland–Altman analysis revealed satisfactory limits of agreement between readers 1 and 2 for each measure at the

Table 2
Interobserver agreement and Bland–Altman analysis for CT parameters at the transverse section line and away from it.

Measure	ICC at transverse section line	ICC away from transverse section line	Bland–Altman analysis at transverse section line	Bland–Altman analysis away from transverse section line
$IWR_{PPP-PVP}$	0.86	0.68	Upper limit: 14.4%, Lower limit: −14.4%	Upper limit: 20.0%, Lower limit: −28.8%
IWR_{PPP-EP}	0.84	0.85	Upper limit: 87.4%, Lower limit: −75.4%	Upper limit: 19.4%, Lower limit: −20.0%
IWR_{PVP-EP}	0.77	0.77	Upper limit: 36.0%, Lower limit: −32.4%	Upper limit: 47.3%, Lower limit: −56.3%
fECV	0.89	0.72	Upper limit: 79.3%, Lower limit: −50.7%	Upper limit: 53.5%, Lower limit: −37.0%

fECV (extracellular volume fraction), *IWR* (iodine washout rate), *PPP* (pancreatic parenchymal phase), *PVP* (portal venous phase), *EP* (equilibrium phase).

Please cite this article as: Fukui H et al., Pancreatic fibrosis assessment and association with pancreatic cancer: comparison with the extracellular volume fraction, Clinical Radiology, https://doi.org/10.1016/j.crad.2024.08.007

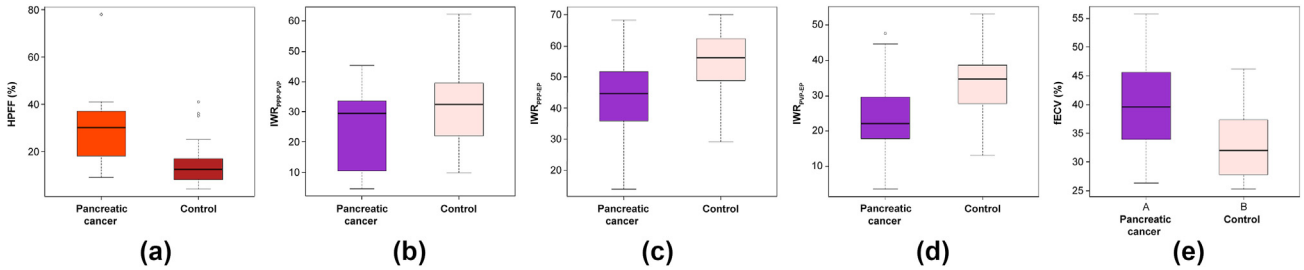

Figure 3 (a) Box plot revealing the median histologic pancreatic fibrosis fraction values being greater in pancreatic cancer group than in the control (30.0% vs. 12.5%; $P<0.01$). (b) Box plot reflecting smaller mean $IWR_{PPP-PVP}$ values in the study group than in the control (25.1% vs. 32.1%; $P<0.05$). (c) Box plot demonstrating the lower mean values of IWR_{PPP-EP} in pancreatic cancer group than in the opposite (43.3% vs. 55.0%; $P<0.01$). (d) Box plot reflecting the mean IWR_{PVP-EP} being lower in the study group than in the counterpart (25.0% vs. 33.5%; $P<0.01$). (e) Box plot displaying the mean fECV (%) having lower values in pancreatic cancer group than in the opposite (40.3% vs. 33.0%; $P<0.01$). *PPP* (pancreatic parenchymal phase), *PVP* (portal-venous phase), *EP* (equilibrium phase), *IWR* (iodine washout rate), and *fECV* (extracellular volume fraction).

transverse section line and away from it (Supplementary Fig 1a–1h). The $IWR_{PPP-PVP}$, IWR_{PPP-EP}, IWR_{PVP-EP}, and fECV values determined by two investigators were averaged for the assessment. Table 3 presents the correlation coefficients between the HPFF and CT parameters, as well as a comparison of these parameters between the pancreatic cancer and control groups. In the 51 patients in whom resected histological specimens could be pathologically analyzed for nonmalignant pancreatic conditions HPFF significantly correlated with the $IWR_{PPP-PVP}$, IWR_{PPP-EP}, IWR_{PVP-EP}, and fECV at the assessed transverse section line [$r = -0.48, -0.69, -0.61$ and -0.65, $P < 0.01$, respectively]. The absolute correlation coefficient had significantly higher values only for IWR_{PPP-EP} than for $IWR_{PPP-PVP}$ ($P < 0.01$). The median HPFF was significantly higher in the pancreatic cancer group than that in the control group (30% vs. 12.5%; $P < 0.01$). The mean values of $IWR_{PPP-PVP}$, IWR_{PPP-EP}, and $IW_{RPVP-EP}$ were significantly lower in the pancreatic cancer group than in the control group (25.1% vs. 32.1%, 43.3% vs. 55.0%, and 25.0% vs. 33.5%, respectively; $P < 0.05$ for $IWR_{PPP-PVP}$ and $P < 0.01$ for IWR_{PPP-EP} and IWR_{PVP-EP}). In contrast, the mean fECV was significantly higher in the pancreatic cancer group compared to the control group (40.3% vs. 33.0%; $P < 0.01$) (Fig 3a–3e). As shown in Table 4, $IWR_{PPP-PVP}$, IWR_{PPP-EP}, IWR_{PVP-EP}, and fECV demonstrated moderate correlations between the transverse section line and the values obtained away from it ($r = 0.74$, 0.74, 0.60, and 0.70, respectively; $P < 0.01$ all). The mean and median values of these parameters did not differ significantly between the two locations ($P > 0.05$ for all comparisons).

We performed a comprehensive linear regression analysis to explore various relationships (Fig 4). The resulting models and their respective coefficients are shown in Table 5. The IWR_{PPP-EP} + fECV and IWR_{PVP-EP} + fECV models generally performed better than the others because they had lower RMSE scores and AIC values. Although there were some differences in the RMSE and AIC values between the DM and non-DM groups, the overall pattern of the model performance remained consistent. The RMSE values for the DM and non-DM groups were comparable to those of the overall cohort, indicating that the models could be applied regardless of the DM status.

The ROC curves received to measure the efficacy of $IWR_{PPP-PVP}$, IWR_{PPP-EP}, IWR_{PVP-EP}, fECV, and linear regression models for estimating pancreatic cancer are demonstrated in Fig 5. A comparison demonstrated significant differences between the DeLong test area under the curve (AUC) of the IWR_{PPP-EP}, IWR_{PPP-EP} + fECV model, and IWR_{PVP-EP} + fECV model and the AUC of the $IWR_{PPP-PVP}$. No significant differences were observed among the other combinations of AUCs.

Discussion

Our findings demonstrated that both IWR, which reflects the kinetics of contrast agent washout, and fECV, which quantifies extracellular matrix accumulation, showed characteristics associated with the extent of fibrosis. This is a pivotal pathological process in various pancreatic conditions.

After administration, contrast agents are distributed throughout intravascular and extracellular–extravascular spaces and rarely penetrate cells.[23] Previous studies using contrast agents have reported that the blood spaces and

Table 4
CT parameters at the transverse section line and away from it: comparison and correlation.

Measure	Transverse section line	Away from transverse section line	Correlation coefficient (r)	P-value (correlation)	P-value (comparison)
$IWR_{PPP-PVP}$	29.2% (SD 13.0)	35.0% (SD 11.8)	0.74	<0.01	0.91
IWR_{PPP-EP}	50.2% (SD 13.3)	53.1% (SD 10.5)	0.74	<0.01	0.214
IWR_{PVP-EP}	29.97% (SD 10.15)	28.23% (SD 7.74)	0.6	<0.01	0.33
fECV	35.99% (IQR, 29.18%–40.21%)	36.48% (IQR, 30.65%–41.88%)	0.7	<0.01	0.7

fECV (extracellular volume fraction), *IWR* (iodine washout rate), *PPP* (pancreatic parenchymal phase), *PVP* (portal venous phase), *EP* (equilibrium phase).

Please cite this article as: Fukui H et al., Pancreatic fibrosis assessment and association with pancreatic cancer: comparison with the extracellular volume fraction, Clinical Radiology, https://doi.org/10.1016/j.crad.2024.08.007

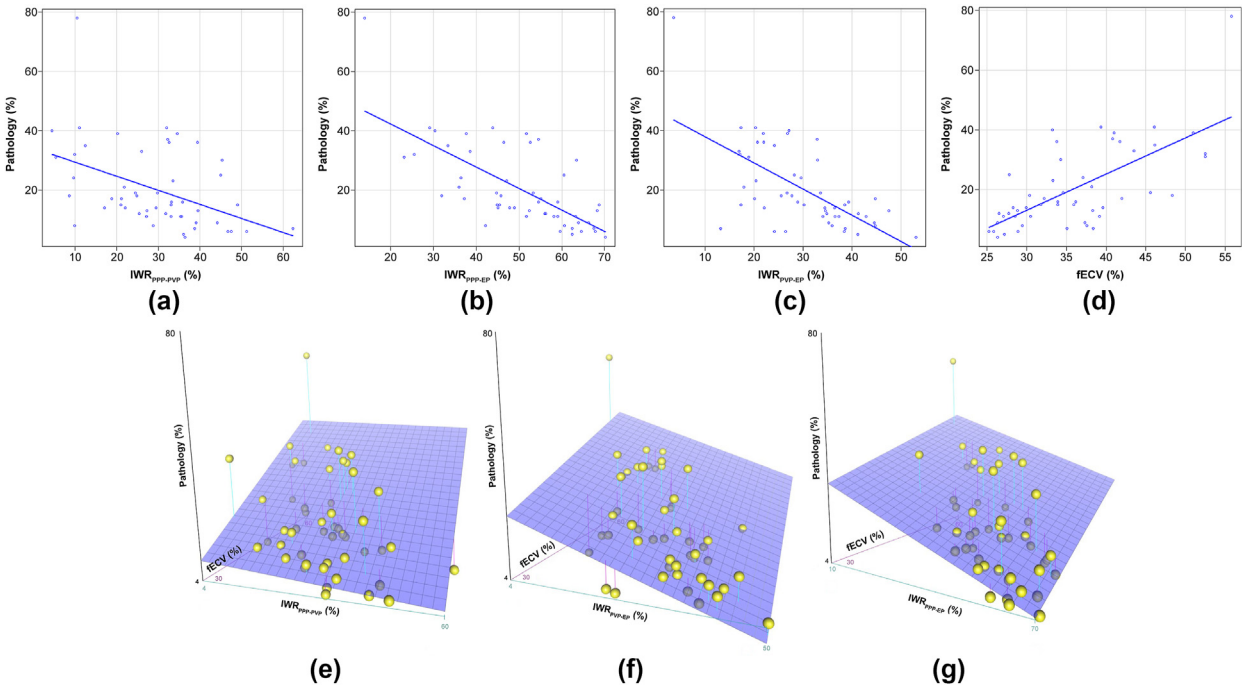

Figure 4 Scatter plots depicting the relationship between pathology (%) and the $IWR_{PPP-PVP}$ (%), IWR_{PPP-EP} (%), IWR_{PVP-EP} (%), and fECV (%). Each plot includes a best-fit simple regression line (a–d). Three-dimensional plots illustrating the best-fit multiple regression planes that relate pathology (%) to combinations of the fECV (%) and $IWR_{PPP-PVP}$ (%), IWR_{PPP-EP} (%), and IWR_{PVP-EP} (%) (e–g). *PPP* (pancreatic parenchymal phase), *PVP* (portal-venous phase), *EP* (equilibrium phase), *IWR* (iodine washout rate), and *fECV* (extracellular volume fraction).

Table 5
Performance of linear regression models for predicting HPFF in the overall cohort, diabetes, and nondiabetes groups.

Model	Equation	RMSE (overall)	AIC (overall)	RMSE (DM)	AIC (DM)	RMSE (Non-DM)	AIC (Non-DM)
$IWR_{PPP-PVP}$ + fECV	Estimate of HPFF = −17.55 + 1.13 × fECV − 0.09 × $IWR_{PPP-PVP}$	10.09	388.49	12.69	257.61	7.77	312.45
IWR_{PPP-EP} + fECV	Estimate of HPFF = 19.05 + 0.65 × fECV − 0.44 × IWR_{PPP-EP}	9.35	380.72	12.02	250.78	6.89	307.32
IWR_{PVP-EP} + fECV	Estimation of HPFF = 6.15 + 0.82 × fECV − 0.51 × IWR_{PVP-EP}	9.23	379.38	10.9	242.67	7.85	298.41
$IWR_{PPP-PVP}$	Estimate of HPFF = 34.23 − 0.48 × $IWR_{PPP-PVP}$	12.36	407.23	15.92	273.12	9.07	325.67
IWR_{PPP-EP}	Estimate of HPFF = 49.36 − 0.54 × IWR_{PPP-EP}	9.94	384.97	12.91	262.01	7.16	313.56
IWR_{PVP-EP}	Estimate of HPFF = 46.77 − 0.88 × IWR_{PVP-EP}	10.57	391.25	12.51	256.89	8.97	309.43
fECV	Estimation of HPFF = −23.25 + 1.21 × fECV	10.13	386.94	12.52	250.12	8.05	304.89

fECV (extracellular volume fraction), *HFPP* (histological pancreatic fibrosis fraction) *IWR* (iodine washout rate), *PPP* (pancreatic parenchymal phase), *PVP* (portal venous phase), *EP* (equilibrium phase), *RMSE* (root mean squared error), *AIC* (Akaike information criterion).

blood flow decreased due to tissues with fibrosis causing a lower volume of contrast influx and delayed clearance of the contrast agent because of slower diffusion between the intravascular and expanded extracellular–extravascular spaces in a pancreatic tissue.[24–26] Therefore, when HPFF showed high values, IWR showed low values, and fECV showed high values. The IWR_{PPP-EP}, IWR_{PVP-EP}, and fECV were significantly correlated with the HPFF, indicating that these imaging metrics could serve as noninvasive markers for assessing pancreatic fibrosis. Several previous studies used CT or magnetic resonance imaging to perform dynamic contrast tests and compared the contrast effects in the pancreatic parenchyma with those in fibrosis.[9,27,28] Hashimoto *et al.* reported that the ratio of mean CT attenuation value (hepatic to pancreatic phase; late/early [L/E] ratio) positively correlated with pancreatic fibrosis.[9] The correlation coefficient between the L/E ratio and HPFF was r=0.75, which is similar to those of our IWR_{PPP-EP} and IWR_{PVP-EP} with HPFF but higher than that of the $IWR_{PPP-PVP}$ with HPFF. In previous reports, several factors accounted for the discrepancies observed: the quantification of histological pancreatic fibrosis was performed in increments of 10%, the measurement location on CT scans differed from the resection margin, and bolus tracking was not used for acquiring PPPs.[9,27,28]

In the comprehensive linear regression analysis in this study, the IWR_{PPP-EP} + fECV and IWR_{PVP-EP} + fECV models exhibited better performance than the others. These models had low AIC[19] and small RMSE[20] values, indicating that the model fit and predictive accuracy were high. By considering the IWR_{PPP-EP} and fECV or IWR_{PVP-EP} and fECV simultaneously, it is possible to predict HPFF more accurately. In addition, our analysis revealed that the performance of our linear regression models was consistent between the DM

Please cite this article as: Fukui H et al., Pancreatic fibrosis assessment and association with pancreatic cancer: comparison with the extracellular volume fraction, Clinical Radiology, https://doi.org/10.1016/j.crad.2024.08.007

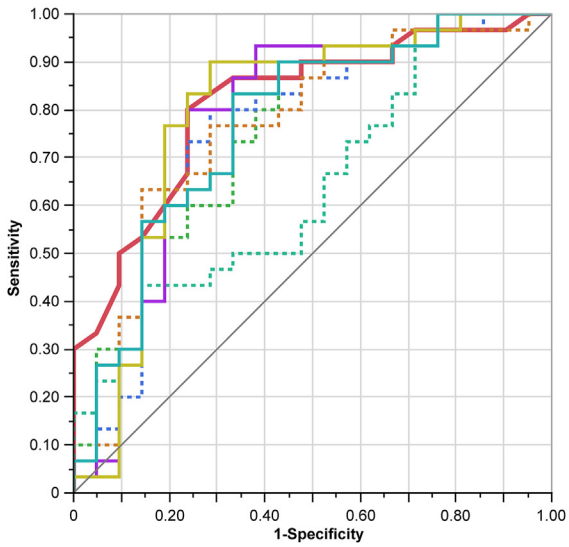

	AUC	Sensitivity	Specificity	Cutoff value
HPFF	0.81	80.0	76.2	17.0
fECV	0.76	90.0	57.2	39.2
IWR_{PPP-EP}	0.75	80.0	71.4	47.8
IWR_{PVP-EP}	0.76	63.3	85.7	33.5
$IWR_{PPP-PVP}$	0.64	43.4	85.7	35.6
IWR_{PPP-EP} + fECV model	0.78	76.7	81.0	18.9
IWR_{PVP-EP} + fECV model	0.79	90.0	71.4	22.7
$IWR_{PPP-PVP}$ + fECV model	0.77	83.3	66.7	23.1

Figure 5 ROC curves obtained to evaluate the efficacy of various parameters in detecting pancreatic cancer, showing AUC, sensitivity, specificity, and the optimal cutoff value. *ROC* (receiver operating characteristic), *AUC* (area under the curve).

and non-DM groups, with RMSE values that were comparable to those of the overall cohort. This finding suggests that our models can be used in a diverse patient population, regardless of the DM status, which should enhance their clinical utility. These regression models may be useful for determining future clinical diagnoses and treatment strategies. In particular, in the diagnosis and staging of pancreatic cancer and even when monitoring treatment effects, these models may be useful.

Patients with pancreatic cancer exhibit pancreatic fibrosis more frequently, and the $IWR_{PPP-PVP}$, IWR_{PPP-EP}, and IWR_{PVP-EP} have low values, whereas fECV has high values because of pancreatic fibrosis. These findings align with the well-established knowledge that pancreatic fibrosis is a precursor to pancreatic cancer.[1–3,29,30] Furthermore, we calculated the cutoff values for the regression model to establish its efficacy in discriminating between pancreatic cancer and control groups. The cutoff values set in this study may be useful for stratifying patients based on a confirmed diagnosis of cancer. $IWR_{PPP-PVP}$, IWR_{PPP-EP}, IWR_{PVP-EP}, and fECV at the estimated cutoff line and the $IWR_{PPP-PVP}$, IWR_{PPP-EP}, IWR_{PVP-EP}, and fECV away from the estimated cutoff line, with no significant differences in the mean and median values. Consequently, the variations in the $IWR_{PPP-PVP}$, IWR_{PPP-EP}, IWR_{PVP-EP}, and fECV have little dependence on the measurement location and are highly reproducible indicators.

This study had several limitations. Pancreatic sections were acquired only from the patients previously subjected to pancreatectomy; thus, the control group had a limited size. Moreover, the study included individuals with long intervals between the intervention and CT imaging, which may have altered the pancreatic fibrosis content. We assessed the equilibrium phase obtained 120 s after PVP acquisition, which is approximately 210 s from the start of contrast-agent administration, to measure the fECV. This time frame may not be enough for the compensation of a contrast agent, although the minimum scan delay time for reliable fECV estimation has not been outlined appropriately. Yoon *et al.*[17] demonstrated that an equilibrium phase of 180 s after contrast injection to assess fECV is a good accommodation of clinical and technical parameters. The retrospective nature of our study and the availability of only a single preoperative CT scan limited our ability to assess the temporal progression of pancreatic fibrosis and its relationship with cancer development. In the future, more factors should be included for analysis.

In conclusion, our study demonstrates that IWR_{PPP-EP}, IWR_{PVP-EP}, and fECV are reliable noninvasive imaging biomarkers for assessing pancreatic fibrosis. A model combining IWR and fECV showed higher accuracy in predicting HPFF than models using each marker alone. Furthermore, we found a significant association between these biomarkers and the presence of pancreatic cancer. However, owing to the limitations of our retrospective study design and the lack of prediagnostic imaging, we could not conclude that changes in pancreatic fibrosis preceded the development of pancreatic cancer. Future prospective longitudinal studies with serial imaging are needed to establish the temporal relationship between pancreatic fibrosis and cancer development, and to assess the utility of these biomarkers for the early detection of pancreatic cancer.

Ethical

Yes.

Funding

No.

Please cite this article as: Fukui H et al., Pancreatic fibrosis assessment and association with pancreatic cancer: comparison with the extracellular volume fraction, Clinical Radiology, https://doi.org/10.1016/j.crad.2024.08.007

Author contribution

Guarantor of integrity of the entire study: Hideyuki Fukui.

Study concepts and design: Hideyuki Fukui, Hiromitsu Onishi.

Literature research: Hideyuki Fukui, Hiromitsu Onishi.

Clinical studies: Hideyuki Fukui, Takashi Ota, Yukihiro Enchi, Daisaku Yamada, Yu Takeda.

Experimental studies/data analysis: Hideyuki Fukui, Daisaku Yamada, Yu Takeda, Takahiro Matsui, Atsushi Nakamoto, Takahiro Tsuboyama.

Statistical analysis: Hideyuki Fukui, Hiromitsu Onishi.

Manuscript preparation: Hideyuki Fukui, Hiromitsu Onishi, Yasunari Fukuda.

Manuscript editing: Noriyuki Tomiyama, Mitsuaki Tatsumi, Shogo Kobayashi, Hidetoshi Eguchi.

Conflict of interest

The authors declare no conflict of interest.

Informed consent

Written informed consent was waived by the Institutional Review Board.

Declaration of generative AI in scientific writing

No.

Acknowledgments

The authors thank Enago (www.enago.jp) for the English-language review. We would like to express our sincere gratitude to Dr. Kazutaka Nishio from the Department of Medical Innovation, Data Coordinating Center, Osaka University Hospital, for their invaluable assistance in performing the statistical analysis. Their expertise and advice greatly contributed to the success of this study.

This work was supported by JSPS KAKENHI Grant Number JP24K18829.

Appendix A. Supplementary data

Supplementary data to this article can be found online at https://doi.org/10.1016/j.crad.2024.08.007.

References

1. Tajima JY, Osada S, Sakuratani T, *et al.* The significance of histopathological evaluation of pancreatic fibrosis to estimate pancreas cancer progression. *Pancreatology* 2016;**16**:S115. https://doi.org/10.1016/j.pan.2016.06.415.
2. Thomas D, Radhakrishnan P. Tumor-stromal crosstalk in pancreatic cancer and tissue fibrosis. *Mol Cancer* 2019;**18**:14. https://doi.org/10.1186/s12943-018-0927-5.
3. Tomita Y, Azuma K, Nonaka Y, *et al.* Pancreatic fatty degeneration and fibrosis as predisposing factors for the development of pancreatic ductal adenocarcinoma. *Pancreas* 2014;**43**:1032–41. https://doi.org/10.1097/MPA.0000000000000159.
4. Sofue K, Ueshima E, Masuda A, *et al.* Estimation of pancreatic fibrosis and prediction of postoperative pancreatic fistula using extracellular volume fraction in multiphasic contrast-enhanced CT. *Eur Radiol* 2022;**32**:1770–80. https://doi.org/10.1007/s00330-021-08255-4.
5. Fukui H, Onishi H, Nakamoto A, *et al.* Pancreatic fibrosis by extracellular volume fraction using contrast-enhanced computed tomography and relationship with pancreatic cancer. *Eur J Radiol* 2022;**156**:110522, https://doi.org/10.1016/j.ejrad.2022.110522.
6. Fukukura Y, Kumagae Y, Higashi R, *et al.* Estimation of extracellular volume fraction with routine multiphasic pancreatic computed tomography to predict the survival of patients with Stage IV pancreatic ductal adenocarcinoma. *Pancreas* 2019;**48**:1360–6. https://doi.org/10.1097/MPA.0000000000001427.
7. Fukukura Y, Kumagae Y, Higashi R, *et al.* Extracellular volume fraction determined by equilibrium contrast-enhanced multidetector computed tomography as a prognostic factor in unresectable pancreatic adenocarcinoma treated with chemotherapy. *Eur Radiol* 2019;**29**:353–61. https://doi.org/10.1007/s00330-018-5570-4.
8. Wang ZJ, Zhang TT, An C, *et al.* Estimation of fractional extracellular space at CT for predicting chemotherapy response and survival in pancreatic ductal adenocarcinoma. *AJR Am J Roentgenol* 2020;**215**:610–6. https://doi.org/10.2214/AJR.19.22462.
9. Hashimoto Y, Sclabas GM, Takahashi N, *et al.* Dual-phase computed tomography for assessment of pancreatic fibrosis and anastomotic failure risk following pancreatoduodenectomy. *J Gastrointest Surg* 2011;**15**:2193–204. https://doi.org/10.1007/s11605-011-1687-3.
10. Nagayama Y, Kato Y, Inoue T, *et al.* Liver fibrosis assessment with multiphasic dual-energy CT: diagnostic performance of iodine uptake parameters. *Eur Radiol* 2021;**31**:5779–90. https://doi.org/10.1007/s00330-021-07706-2.
11. Working Group IAP/APA Acute Pancreatitis Guidelines. IAP/APA evidence-based guidelines for the management of acute pancreatitis. *Pancreatology* 2013;**13**:e1–15. https://doi.org/10.1016/j.pan.2013.07.063.
12. American Diabetes Association Professional Practice Committee. 2. Diagnosis and classification of diabetes: standards of care in diabetes-2024. *Diabetes Care* 2024;**47**:S20–42. https://doi.org/10.2337/dc24-S002.
13. Fukuda Y, Yamada D, Eguchi H, *et al.* CT density in the pancreas is a promising imaging predictor for pancreatic ductal adenocarcinoma. *Ann Surg Oncol* 2017;**24**:2762–9. https://doi.org/10.1245/s10434-017-5914-3.
14. Yokoyama T, Lee JK, Miwa K, *et al.* Quantification of sympathetic hyperinnervation and denervation after myocardial infarction by three-dimensional assessment of the cardiac sympathetic network in cleared transparent murine hearts. *PLOS ONE* 2017;**12**:e0182072, https://doi.org/10.1371/journal.pone.0182072.
15. Sin J, Puccini JM, Huang C, *et al.* The impact of juvenile coxsackievirus infection on cardiac progenitor cells and postnatal heart development. *PLOS Pathog* 2014;**10**:e1004249, https://doi.org/10.1371/journal.ppat.1004249.
16. Shinagawa Y, Sakamoto K, Sato K, *et al.* Usefulness of new subtraction algorithm in estimating degree of liver fibrosis by calculating extracellular volume fraction obtained from routine liver CT protocol equilibrium phase data: preliminary experience. *Eur J Radiol* 2018;**103**:99–104. https://doi.org/10.1016/j.ejrad.2018.04.012.
17. Yoon JH, Lee JM, Klotz E, *et al.* Estimation of hepatic extracellular volume fraction using multiphasic liver computed tomography for hepatic fibrosis grading. *Invest Radiol* 2015;**50**:290–6. https://doi.org/10.1097/RLI.0000000000000123.
18. Meng XL, Rosenthal R, Rubin DB. Comparing correlated correlation coefficients. *Psychol Bull* 1992;**111**:172–5. https://doi.org/10.1037/0033-2909.111.1.172.
19. Akaike H. A new look at the statistical model identification. *IEEE Trans Autom Control* 1974;**19**:716–23. https://doi.org/10.1109/TAC.1974.1100705.
20. Chai T, Draxler RR. Root mean square error (RMSE) or mean absolute error (MAE)? – arguments against avoiding RMSE in the literature. *Geosci Model Dev* 2014;**7**:1247–50. https://doi.org/10.5194/gmd-7-1247-2014.

21. Akobeng AK. Understanding diagnostic tests 3: receiver operating characteristic curves. *Acta Paediatr* 2007;**96**:644–7. https://doi.org/10.1111/j.1651-2227.2006.00178.x.
22. Bland JM, Altman DG. Measuring agreement in method comparison studies. *Stat Methods Med Res* 1999;**8**:135–60. https://doi.org/10.1177/096228029900800204.
23. Currie GM. Pharmacology, Part 5: CT and MRI contrast media. *J Nucl Med Technol* 2019;**47**:189–202. https://doi.org/10.2967/jnmt.118.220012.
24. Lewis MPN, Lo SK, Reber PU, *et al*. Endoscopic measurement of pancreatic tissue perfusion in patients with chronic pancreatitis and control patients. *Gastrointest Endosc* 2000;**51**:195–9. https://doi.org/10.1016/s0016-5107(00)70417-2.
25. Uhlmann D, Ludwig S, Geissler F, *et al*. Importance of microcirculatory disturbances in the pathogenesis of pancreatitis. *Zentralbl Chir* 2001;**126**:873–8. https://doi.org/10.1055/s-2001-19157.
26. Arikawa S, Uchida M, Kunou Y, *et al*. Assessment of chronic pancreatitis: use of whole pancreas perfusion with 256-slice computed tomography. *Pancreas* 2012;**41**:535–40. https://doi.org/10.1097/MPA.0b013e3182374fe0.
27. Tajima Y, Matsuzaki S, Furui J, *et al*. Use of the time–signal intensity curve from dynamic magnetic resonance imaging to evaluate remnant pancreatic fibrosis after pancreaticojejunostomy in patients undergoing pancreaticoduodenectomy. *Br J Surg* 2004;**91**:595–600. https://doi.org/10.1002/bjs.4461.
28. Tajima Y, Kuroki T, Tsuneoka N, *et al*. Monitoring fibrosis of the pancreatic remnant after a pancreaticoduodenectomy with dynamic MRI. *J Surg Res* 2010;**158**:61–8. https://doi.org/10.1016/j.jss.2008.07.033.
29. Huang C, Iovanna J, Santofimia-Castaño P. Targeting fibrosis: the bridge that connects pancreatitis and pancreatic cancer. *Int J Mol Sci* 2021;**22**:4970. https://doi.org/10.3390/ijms22094970.
30. Malka D, Hammel P, Maire F, *et al*. Risk of pancreatic adenocarcinoma in chronic pancreatitis. *Gut* 2002;**51**:849–52. https://doi.org/10.1136/gut.51.6.849.

Please cite this article as: Fukui H et al., Pancreatic fibrosis assessment and association with pancreatic cancer: comparison with the extracellular volume fraction, Clinical Radiology, https://doi.org/10.1016/j.crad.2024.08.007